

Articles

Polymer Coating of Steel by a Combination of Electrografting and Atom-Transfer Radical Polymerization

M. Claes,[†] S. Voccia,[†] C. Detrembleur,[†] C. Jérôme,[†] B. Gilbert,[‡] Ph. Leclère,[§]
V. M. Geskin,[§] R. Gouttebaron,[⊥] M. Hecq,[⊥] R. Lazzaroni,[§] and R. Jérôme^{*,†}

Center for Education and Research on Macromolecules (CERM), Centre de Recherche en Science des Matériaux Polymères (CRESMAP), Université de Liège, B6 Sart-Tilman, B-4000 Liège, Belgium, Laboratory of Analytical Chemistry and Electrochemistry, Université de Liège, B6 Sart-Tilman, B-4000 Liège, Belgium, Service de Chimie des Matériaux Nouveaux, Centre de Recherche en Science des Matériaux Polymères (CRESMAP), Université de Mons-Hainaut, Place du Parc 20, B-7000 Mons, Belgium, and Service de Chimie Inorganique et Analytique (L.A.S.S.I.E.), Université de Mons-Hainaut, Place du Parc 20, B-7000 Mons, Belgium

Received November 26, 2002; Revised Manuscript Received June 3, 2003

ABSTRACT: Cathodic electrografting of poly(2-chloropropionate ethyl acrylate) (poly[cPEA]) onto steel followed by the styrene grafting-from by atom transfer radical polymerization (ATRP) is an efficient strategy to impart strong adhesion to polystyrene films onto the electrically conductive substrate. Electrografting of poly(cPEA) chains at an appropriate potential and persistence of the activated chloride in the grafted chains were confirmed by XPS. Polystyrene deposition by ATRP with a ruthenium-based catalyst was analyzed by scanning electron microscopy and Raman spectroscopy. Adhesion of the polystyrene layer to the substrate is so strong that it cannot be detached by standard Scotch brand tapes. Moreover, local thermal analysis showed a loss of mobility for the PS chains tethered at the surface.

Introduction

Nowadays, the surface of a variety of organic and inorganic substrates is coated by synthetic polymers in order to impart them specific properties (e.g., adhesion, hydrophilicity or hydrophobicity, low friction, resistance to environmental attack, etc.). The major problem to be tackled is however the usually weak and short-term adhesion between organic polymers and completely different materials, e.g., metals, glass, and carbon. Covalent bonding at the interface is by far the more desirable situation.^{1,2} In this respect, electropolymerization of (meth)acrylates proved to be a powerful tool to deposit polymers strongly adhering to electrically conducting substrates.^{3–5} At an appropriate potential, the electroreduction of these monomers leads to the rapid formation of an insulating film on the cathode whatever its shape (plate, fiber) and nature (metal, carbon, indium tin oxide glass).^{6,7} This strategy, however, has limitations. Indeed the film thickness is small (<100 nm)⁸ as result of the fast passivation of the cathode, and the monomers which can be electrografted are restricted to one (although large) family of monomers, i.e., (meth)acrylates.⁵ Moreover, any organic function in the ester group (e.g., protic amine, carboxylic

acid) which can be reduced at the electrografting potential cannot be tolerated.

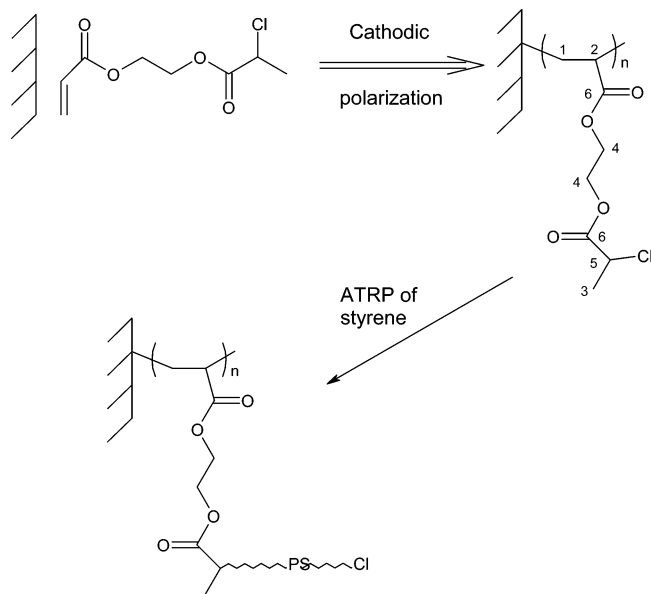
A valuable way to tackle this problem is to combine the electrografting technique and a living/controlled polymerization reaction. This type of approach should indeed allow films of polymers other than poly(meth)acrylates to be deposited on conducting substrates with strong adhesion and increased thickness. The basic idea is to have (meth)acrylates bearing an initiator of living/controlled polymerization in the ester group electrografted onto the solid surface without modification of the pendant group. In a recent paper,⁹ Detrembleur et al. reported on the electrografting of norbornenylmethacrylate. In a second step, the norbornenyl pendant groups were added with the Grubbs¹⁰ catalyst and used to successfully initiate the “living” ring opening metathesis polymerization (ROMP) of norbornene. Strongly adhering homogeneous poly(norbornene) films were accordingly deposited on various substrates and proved to be very efficient in protecting steel against corrosion. More recently, Voccia et al.¹¹ reported on the combination of the electrografting technique with the nitroxide mediated radical polymerization (NMP). This combination allowed polystyrene films to be grown at the surface of conducting substrates (carbon, steel). The NMP of styrene being well-controlled, the thickness of the films, i.e., M_n of polystyrene, was controlled by the addition of free alkoxyamine to the polymerization solution, in which the substrate is immersed. Although successful, the scope of this method might be limited by the tedious synthesis of alkoxyamine-containing

[†] Centre de Recherche en Science des Matériaux Polymères (CRESMAP), Université de Liège.

[‡] Laboratory of Analytical Chemistry and Electrochemistry, Université de Liège.

[§] Centre de Recherche en Science des Matériaux Polymères (CRESMAP), Université de Mons-Hainaut.

[⊥] Service de Chimie Inorganique et Analytique (L.A.S.S.I.E.), Université de Mons-Hainaut.

Scheme 1. Two-Step Process for the Grafting from of Polystyrene from an Electrically Conducting Substrate

acrylates and the intrinsic limitations of NMP (restricted range of monomers and high temperature).

Recent developments in atom transfer radical polymerization (ATRP) paved the way to the synthesis of new polymeric materials and composites.^{12–16} Because ATRP is tolerant of a variety of functional groups (alcohol, amine, carboxylic acid, sulfonate), a combination of electrografting with ATRP might be a more general approach than the strategies based on ROMP and NMP, respectively.

In this paper, we report on the synthesis of 2-chloropropionyl ethyl acrylate (cPEA), i.e., an easily prepared dual monomer bearing an acrylate function prone to be electrografted and an activated chloride able to initiate the controlled radical polymerization of vinyl monomers by ATRP (Scheme 1). This monomer was electrografted on steel, a non-noble metal, with formation of a strongly adhering macroinitiator for the ATRP of styrene. This coating was characterized by XPS and then used to initiate the polymerization of styrene with the purpose to compare the potential of ATRP with the previously tested NMP. Polystyrene films of tunable thickness were prepared by grafting from the surface of the cPEA-modified steel. Adhesion was estimated by peeling tests, and the mobility of the grafted chains was characterized by local thermal analysis.

Experimental Part

Materials. The monomer (cPEA) was dried over molecular sieves before electropolymerization, and the comonomer, ethyl acrylate (EA), was dried over calcium hydride and distilled under reduced pressure. *N,N*-Dimethylformamide (DMF) was dried over P_2O_5 and distilled under reduced pressure. Tetraethylammonium perchlorate (TEAP) was heated in vacuo at 80 °C for 12 h, prior to use. Styrene (Aldrich) was dried over CaH_2 and distilled before use. Phenylethyl bromide (PEBr) (Aldrich) and HMTETA (Aldrich) were diluted in dried toluene. The Grubbs catalyst (Aldrich) and $NiBr_2(PPh_3)_2$ (Aldrich) were used as received, and CuCl (Aldrich) and $CuCl_2$ (Aldrich) were purified by recrystallization in acetic acid, before use.

Synthesis. cPEA was prepared by reaction of 10 mL of 2-chloropropionyl chloride (0.1 mol dissolved in 20 mL of THF) with 5.74 mL of 2-hydroxyethyl acrylate (0.05 mol) and 6.97 mL of triethylamine (0.05 mol) dissolved in 60 mL of dried

THF. Then, 20 h later, the triethylamine hydrochloride byproduct was filtered out and washed with THF. Upon THF evaporation from the filtrate, a liquid residue was left, extracted by $CHCl_3$, washed three times with water, eluted through a silica gel column by $CHCl_3$, and dried over $MgSO_4$. After distillation, cPEA was recovered with an 82% yield. The structure of the monomer was confirmed by 1H NMR and IR spectroscopy.

1H NMR ($CDCl_3$): δ = 1.68 (d, 3H), 4.41 (m, 5H), 5.89 (d, 1H), 6.14 (q, 1H), 6.46 (d, 1H).

IR (NaCl): (cm^{-1}) 2962, 1730, 1620, 1637, 1175.

The styrene polymerization was performed in closed tubes under nitrogen. In a 1.5 cm diameter tube was added 68 mg (0.082 mmol for a targeted DP = 950) of the Grubbs catalyst, together with the electrografted steel plate in a vertical position. The tube was closed by a three-way stopcock, evacuated and filled with nitrogen. Then, 2 mL of dry toluene, 9 mL of styrene (78.5 mmol) and 0.23 mL of PEBr (0.082 mmol; targeted DP = 950) were then added through a rubber septum making the steel plate completely immersed. The tube was placed on a magnetic stirrer (the magnetic steel plate being the stirring bar) and heated at 100 °C for 18 h. After polymerization, the steel plate was extensively washed with THF, and the polymer formed in solution was recovered by precipitation in methanol.

For an analytical purpose, the ester bonds of poly(cPEA) were hydrolyzed by NaOH (1 M solution in THF) for 24 h. The accordingly released PS was precipitated in methanol and analyzed by SEC.

Characterization. Cyclic voltammetry (CV) was carried out in *N,N*-dimethylformamide containing TEAP (5×10^{-2} M) as the conducting salt, at a scanning rate of 20 mV/s. The water content of the medium was measured by the Karl Fischer method (Tacussel aquaprocessor) and ascertained to be lower than 5 ppm. All the electrochemical experiments were carried out in a glovebox under an inert and dry atmosphere, at room temperature. Both the electrochemical cell and preparation of the cathode were detailed elsewhere.¹⁷ Briefly, the steel electrode (1×1 cm) was cleaned by heptane and acetone, and the superficial oxide layer was electrochemically reduced in acetonitrile before electrografting. Because of the drastic anhydrous conditions required by the electrografting reaction, the use of a conventional reference electrode was precluded, and the potentials were measured against a Pt pseudo-reference making the potentials recorded in solutions of different compositions not directly comparable.

Size exclusion chromatography (SEC) was carried out with a THF/triethylamine (5 wt % of triethylamine) solution at 40 °C using a Waters 600 liquid chromatograph. It was equipped with a 410 refractive index detector and Styragel HR columns (HR 1, 100–5000; HR2, 500–20000; HR4, 5000–600000), that were calibrated with PS standards.

Raman spectroscopy was carried out with a Dilor spectrometer (SuperLabram type), equipped with a liquid nitrogen-cooled 800–2000 CCD detector and a microscope. The spectral resolution was 2 cm^{-1} . The excitation laser beam was focused on the sample via the microscope. The analysis spot size was smaller than $1\text{ }\mu\text{m}$, and the analysis area was ca. $1\text{ }\mu\text{m}^2$ when the $100\times$ lens was used. However, the spectra were independent of the location of the spot, which confirmed the film homogeneity. Because of the dispersion of the grating and the use of a 1 in. CCD detector, the full spectrum had to be recorded in two parts (first range, 200–1800 cm^{-1} ; second range, 2400–3700 cm^{-1}).

XPS analysis was performed with a VG-ESCALAB 220iXL spectrometer. The pressure in the analysis chamber was typically 8×10^{-11} Torr. The XPS data were collected using monochromatized Al K α radiation at 1486.6 eV. Photoelectrons were collected from a $250 \times 1000\text{ }\mu\text{m}^2$ sample area at takeoff angles of $\vartheta = 0^\circ$ (normal detection) and $\vartheta = 46^\circ$ (grazing detection). In addition to survey spectra (50 eV pass energy), high-resolution spectra were recorded in the regions of C 1s, O 1s, Cl 2p, Fe 2p, and Si 2p with a 20 eV pass energy. Atomic composition was derived from the peak areas by using the photoionization cross sections calculated by Scofield, corrected

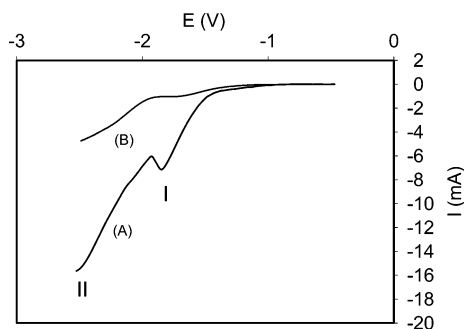


Figure 1. Cyclic voltammograms recorded onto steel in DMF containing 0.05 M TEAP and (A) 0.5 M cPEA or (B) 0.5 M cPB.

for the dependence of the escape depth (λ) on the kinetic energy of the electrons (E) (of the form $I = KE^{0.6}$) and corrected for the analyzer transmission function of the spectrometer. The modified substrates were washed with DMF and acetonitrile, then dried under vacuum at 80 °C over one night in order to remove the high boiling point DMF, which was observed by XPS at a similar energy as for our product (C=O amide and ester). However, this drying step was responsible for contamination by silicon residues released by the oil–vacuum pump. These silicone peaks appeared however at lower energy, such that the grafting of the ester derivative could be confirmed.

Scanning electron microscopy (SEM) was performed with an Explorer scanning electron microscope.

A μ TA 2290 microthermal analyzer (TA Instruments) equipped with a TopoMetrix Explorer TMX2100 scanning probe microscope was used for microthermal analysis. In the imaging mode, the displacement of the tip in contact with the heated sample was measured. At selected locations, the temperature was raised, typically at a 5 °C/s rate, and the power at the tip was compared with a similar tip left in air. Temperature was scanned up to 200 °C, and the temperature scale was calibrated with a sample of Polyamide 6 (melting temperature: 202 °C). To increase the sensitivity, the temperature ramp was modulated by a 5 kHz signal with an amplitude of 2 °C. Because of the low thermal conductivity of polymers, the thermal properties were probed on a local scale of ca. 10 μm^3 . Measurements were repeated at different locations in order to check the homogeneity of the samples.

Results and Discussion

The concept of combining electropolymerization and ATRP was validated by using a dual monomer, i.e., an acrylate known for propensity to electrografting, that contains an ATRP initiator in the ester group. Rather than an activated bromide commonly used to initiate ATRP, a chlorinated monomer, i.e., 2-chloropropionate ethyl acrylate (cPEA), was selected because of a higher stability under cathodic potential (Scheme 1). This dual monomer was synthesized with high yield (82%), by reaction of 2-hydroxyethyl acrylate with 2-chloropropionyl chloride in the presence of triethylamine.

The very first step of the process is the electrografting of the new cPEA monomer onto the cathode. Figure 1 shows the voltammograms recorded for the cPEA reduction (0.5 M) onto steel in DMF containing tetraethylammonium perchlorate (TEAP; 0.05 M). The curve shows the two distinct phenomena commonly observed for the electroreduction of acrylates,¹⁸ i.e., a low intensity peak at the less cathodic potential (peak I) which is the signature of the polymer grafting (passivation peak) and a more cathodic peak of much higher intensity (peak II), which is characteristic of the monomer reduction into species that initiate polymerization in solution concomitant with the degrafting of the chains formed at peak I.¹⁸

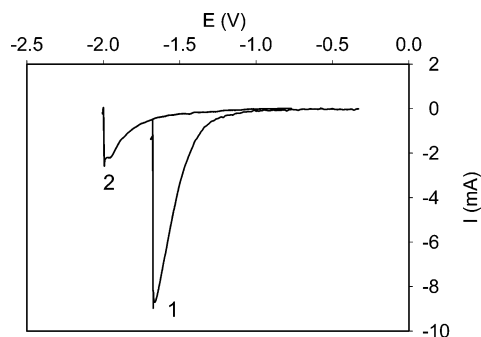


Figure 2. Cyclic voltammograms for EA/cPEA mixtures (1 M) of various molar compositions: (1) 50/50; (2) 90/10. Both were recorded onto steel in DMF containing TEAP (0.05 M).

Table 1. Potential and Current Density of Peak I for the Cathodic Reduction of CPEA/EA Mixtures of Different Compositions

cPEA/EA monomer ratio in solution	E (V) first peak	I (mA) first peak
100/0	-1.8	-9
50/50	-1.7	-8
10/90	-2	-2
0/100	-2.1	-0.25

The stability of the C–Cl bond of cPEA under cathodic potential was tested with a non polymerizable model compound, 1-butyl chloropropionate (cPB). Curve B in Figure 1 shows a very weak current at the potential of the grafting peak, which increases when the potential goes beyond -2 V. This electrochemical reaction is attributed to the cleavage of the activated C–Cl bond with formation of chloride anion and a carbon radical. Although the electroreduction of the activated C–Cl bond mainly occurs at potentials more cathodic than -2 V, this reaction cannot be completely ruled out at the potential of the grafting peak. Nevertheless, the huge difference in intensity between the reduction current of C–Cl and peaks I indicates the predominance of electrografting over the side reaction of chloride.

Copolymerization of cPEA with an alkyl acrylate is a possible way to modulate the chlorine content of the grafted film and to limit further the extent of the interfering C–Cl reaction. Ethyl acrylate (EA) is known for easy electrografting onto steel in DMF solution.¹⁹ Figure 2 shows the voltammograms recorded for mixtures of EA and cPEA at constant 1 M concentration. As reported in Table 1, the intensity of the grafting peak is lower for EA than for cPEA, which suggests a stronger adsorption of cPEA to the electrode and accordingly a lower polymerization rate and delayed passivation. Moreover, the grafting potential is slightly more cathodic in the case of EA. 10% cPEA is enough to increase the current intensity by an order of magnitude, which indicates a preferential adsorption of cPEA to the electrode and expectedly a higher cPEA content in the film compared to the comonomer feed.

In agreement with previous observations, e.g., for acrylonitrile and ethyl acrylate, the electrode is almost completely passivated when the scanning of the cathodic potentials is stopped at the maximum of peak I, thus after a few seconds. Indeed, the intensity of peak I is strongly reduced when the potential is scanned for the second time (Figure 3). This passivation results from the chemisorption of an insulating polyacrylate film on the conducting surface, even when the experiment is conducted in a good solvent for the polymer. Because a Pt pseudo-reference was used in all the electrochemical

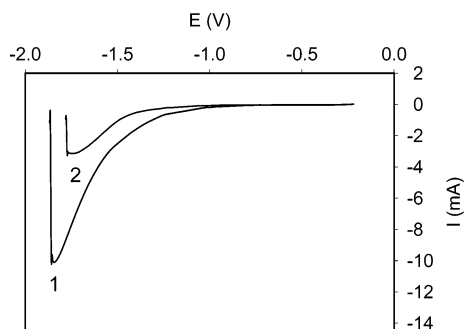


Figure 3. Cyclic voltammograms recorded in DMF containing 0.05 M TEAP and 0.5 M cPEA onto steel: (1) first scan; (2) second scan.

experiments, the potential value of the maximum of peak I in Figure 3 cannot be compared to the ones in Figure 2 recorded for solutions of different composition.

Steel cathodes were electrografted by poly(cPEA) and poly(cPEA-co-EA) from 0.5 M monomer(s) solution in DMF, by scanning the potential up to the maximum of the first peak and holding this potential until the current decreases dramatically. The cathode passivation was completed by a second potential scan. The electrodes were then carefully washed with pure DMF (a solvent for the (co)polymer) and acetonitrile, and dried. The electrodeposited poly(cPEA) and poly(cPEA-co-EA) films were too thin to be visible by the naked eye. They were therefore analyzed by X-ray photoelectron spectroscopy (XPS). Figure 4A shows the wide energy scan spectrum recorded for a poly(cPEA) film. One main peak is observed for each component of the organic film, i.e., oxygen, carbon, and chlorine. Two additional peaks at low energy, characteristic of silicon, indicate contamination of the sample surface by silicone residues released by the oil–vacuum pump used during drying. Because no peak characteristic of iron is detected, the steel surface is completely covered by an organic film thicker than 10 nm (which is the typical depth probed by XPS). The analysis of the energy range between 283 and 291 eV (C 1s area, Figure 4B) allows discriminating several components for carbon atoms in different environments. The assignment of these peaks is reported in Table 2, together with the experimental atomic ratios and the theoretical values expected for poly(cPEA). Except for the component at low energy (285.0 eV), which is much too intense, there is a good agreement between theory and experiment. The excess of carbon at low energy is the signature of hydrocarbon and silicone contamination. It must be noted that the experimental ester carbon/chlorine atomic ratio is 2.2, thus 10% higher than the theoretical value. The loss in chlorine during the monomer reduction is thus limited to ca. 10%.

The XPS analysis of the copolymers also shows all the expected peaks (C, O, Cl). However, an iron signal is observed for samples electrodeposited onto steel (normal geometry), which indicates that the films are either thinner or nonuniform compared to the cPEA films. Film thickness can be approximated from the attenuation of the iron signal on the assumption that the film is uniform. Values of 9.9 and 8.4 nm were calculated for copolymers containing 50 and 10% cPEA, respectively. On the basis of the inelastic mean free path of Fe 2p electrons through an organic matrix ($\lambda(\text{Fe } 2p) = 2.7 \text{ nm}$), an organic film thickness higher or equal to 8.1 nm (i.e., 3 times $\lambda(\text{Fe } 2p)$) deposited onto the substrate should completely mask the Fe 2p signal. The

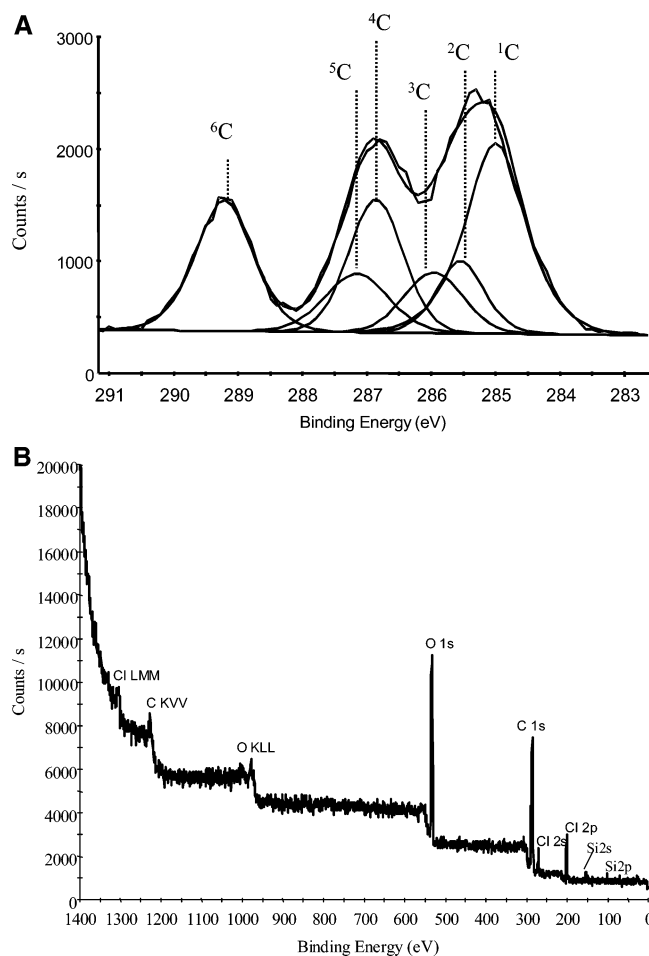


Figure 4. XPS spectrum of poly(cPEA) electrografted onto steel: (A) general spectrum; (B) carbon range and fitting.

Table 2. Atomic Ratios for the Poly(cPEA) Film Measured by XPS by Fitting the Carbon Peak Area^a

bonding energy (eV)	expected area ratio	experimental area ratio	atomic %
285 (¹ C–C _∞)	1	2.9	21.2
285.6 (² C–COO)	1	1	6.6
285.9 (³ C–CCl)	1	1	6.6
287 (O– ⁴ C–C)	2	2	13.5
287.2 (OOC– ⁵ CCl)	1	1	6.6
289.2 (⁶ COO)	2	2	13.3
200.6 (Cl)	1	0.9	5.9

^a Comparison with the ratios expected for the neat polymer.

estimated thicknesses however exceed this threshold value. Moreover, if the iron signal is not observed in the most surface-sensitive mode (grazing geometry) because the electrons are of a low kinetic energy, the O 1s signal at 530.2 eV characteristic of iron oxide remains detected. Therefore, the picture of a nonuniform coating emerges, with “spots” of copolymer leaving part of the surface uncoated. The composition of the organic layer depends on the angle used for analysis (Table 3). The chlorine content is higher in the depth of the coating rather than at the extreme surface, which is consistent with the preferential adsorption of cPEA compared to EA suggested by voltammetry. The Cl 2p spectrum shows two components at 200.6 eV (C–Cl bond) and 198.8 eV (Cl[−] anions released by reduction), with a 0.85/0.15 atomic ratio. For the 50/50 sample, the composition of the film is close to the composition of the comonomer solution, the C ester/Cl ratio being 3.1 (i.e., very close to 3). However, for the 90/10 sample, the ratio is much

Table 3. Atomic Contents for Poly(cPEA) Homopolymer and Copolymers Measured by XPS with the Normal and Grazing (Angle of 46° from the Normal) Geometries

cPEA/EA in solution	Fe	O	C	Cl	Si
100/0		25.8	65.8	5.9	2.5
50/50					
normal geometry	0.5	25.1	65.8	3.8	4.9
grazing geometry	<0.1	25.6	67.3	2.0	5.0
10/90					
normal geometry	0.7	28.9	64.9	5.5	
grazing geometry	<0.1	28.4	68.1	3.5	

lower than expected (2.4 instead of 11), which confirms that cPEA is preferentially incorporated, as was tentatively concluded from voltammetric data in Table 1. It thus appears that copolymerization of cPEA with EA does not allow to tune much the content of activated chlorine in the film, because of the preferential adsorption of cPEA at the cathode. Moreover, the uniformity of the poly(cPEA) films is lost when cPEA is copolymerized with EA in DMF.

Poly(cPEA) modified electrodes were used as macro-initiators for the styrene polymerization by ATRP. They were dipped in a mixture of toluene (2 mL) and styrene (9 mL) in the presence of the ATRP catalyst for 18 h under nitrogen. The catalytic system developed by Matyjaszewski and al. (CuCl/CuCl₂/HMTETA)¹² was first used, because of the good control imparted to the styrene polymerization both in solution¹² and from various solid surfaces.²⁰ However, in this study, the metallic substrate (steel) is rapidly corroded by Cu(II), which prompted us to use the commercially available Grubbs catalyst (RuCl₂(=CHPh)(PCy₃)₂), known for control of the styrene radical polymerization^{21–23} and inertness toward steel. Polystyrene was then successfully “grafted-from” the surface of poly(cPEA) modified steel. For analytical purpose, it was recovered by hydrolysis of the ester bonding PS to poly(cPEA) and analyzed by SEC (Table 4, entry 1). To decrease the molecular weight of the grafted PS chains, and thus the PS film thickness, various amounts of phenylethyl bromide (PEBr) were added to the polymerization medium (Table 4, entries 2, 3, and 4). Whenever the amount of PEBr is increased, the molecular weight of grafted PS is decreased. Moreover, nongrafted polystyrene is formed in solution whatever the polymerization conditions. Discrepancy between theoretical and experimental M_n and high polydispersity show that the styrene polymerization is not well controlled by the Grubbs catalyst. The grafted chains are also of higher molecular weight and polydispersity than the nongrafted ones (Table 4). The main reason for this poor control has to be found in a styrene metathesis side-reaction which occurs when the ATRP of styrene is conducted with the Grubbs catalyst. This competing reactions went however unobserved until now.^{21–23} In this work, whenever styrene was grafted from the

surface of poly(cPEA) modified steel, gas bubbles were noted during the first minutes of reaction, which is not the case in the presence of the copper catalyst. The most reasonable explanation for this observation is that polyaddition of styrene by ATRP is challenged by metathesis of styrene into stilbene and gaseous ethylene. This hypothesis was assessed by the analysis of the polymerization medium by GC–MS. A compound with a molecular weight of 180 was observed and identified as stilbene by ¹H NMR. The use of an internal standard allowed the stilbene formation to be estimated at 1.5 to 1.7 wt % during the first stage of the polymerization. To improve the control of the styrene polymerization, NiBr₂(PPh₃)₂ was substituted for the Grubbs catalyst. Although the metathesis reaction is avoided, the molecular weight distribution remains broad (Table 4, entry 5). According to the scientific literature, the most efficient catalyst for the styrene ATRP is the copper catalyst.¹² Therefore, the “grafting-from” of styrene was repeated with the CuCl/CuCl₂/HMTETA catalytic system and poly(cPEA) electrografted onto vitreous carbon plate instead of steel (Table 4, entry 6). Vitreous carbon is indeed inert toward copper cations which is not the case for iron, as observed in previous experiments. The agreement between M_n for the grafted PS chains and PS formed in solution is the best ever observed in this work, and the polydispersity is low as it must be.

After careful washing with THF, a good solvent for polystyrene, the surface was analyzed by FTIR–RAS and Raman spectroscopy. The recorded spectra were basically the same as those recorded for solvent-cast polystyrene, which confirms that the surface is coated by a stable PS layer. Because the film thickness is smaller than the depth of analysis by Raman, the intensity of the signals is proportional to the film thickness. This intensity of the signal for the aromatic rings at 1000 cm^{−1} was measured under identical conditions (power of the laser, aperture, number of scans, ...) and plotted vs M_n of PS measured by SEC after hydrolysis. Figure 5 shows a linear dependence of the Raman signal intensity on M_n of PS, which indicates that the film thickness can be predetermined by the PS chain length, thus the styrene/PEBr molar ratio. This chain length is now under good control.

As indirect evidence of the successful “grafting from” of polystyrene initiated by the poly(cPEA) coating (whatever the solid substrate), the experiment was repeated with bare steel plates. No polymer was deposited on the substrate after 18 h of immersion in a solution of the ATRP catalyst in styrene. Similarly, no polystyrene was deposited for electrodes premodified by the electroreduction of the model compound (cPB) instead of the cPEA monomer. Clearly, styrene is polymerized from the solid surface only when an activated halide is attached to it by electrografting.

Table 4. M_n and Polydispersity of Grafted and Nongrafted PS Chains As Measured by SEC in THF

entry	grafted polymer	$T(^{\circ}\text{C})$	time (h)	amount of PEBr (mmol)	targeted M_n (conversion 100%)	M_n of grafted PS	polydispersity of grafted PS	M_n of PS in solution	polydispersity of PS in solution
1	P(cPEA)	110	18	0		345 000	4.1	225 000	2.05
2	P(cPEA)	110	18	2.8×10^{-2}	470 000	297 000	3.9	170 000	3.3
3	P(cPEA)	110	18	8.25×10^{-2}	143 000	148 000	3.4	97 000	1.95
4	P(cPEA)	110	18	4.1×10^{-1}	28 000	17 000	7.4	4000	1.55
5	P(cPEA) ^a	110	18	2.8×10^{-2}	470 000	220 000	3.3	155 000	2.75
6	P(cPEA) ^b	110	18	5.3×10^{-2}	115 000	160 000	1.5	140 000	1.4
7	P(cPEA-co-EA) 50:50	110	18	8.25×10^{-2}	95 000	92 000	7.0	83 000	1.65

^a Experiment performed with NiBr₂(PPh₃)₂ on steel. ^b Experiment performed with CuCl/CuCl₂ on vitreous carbon.

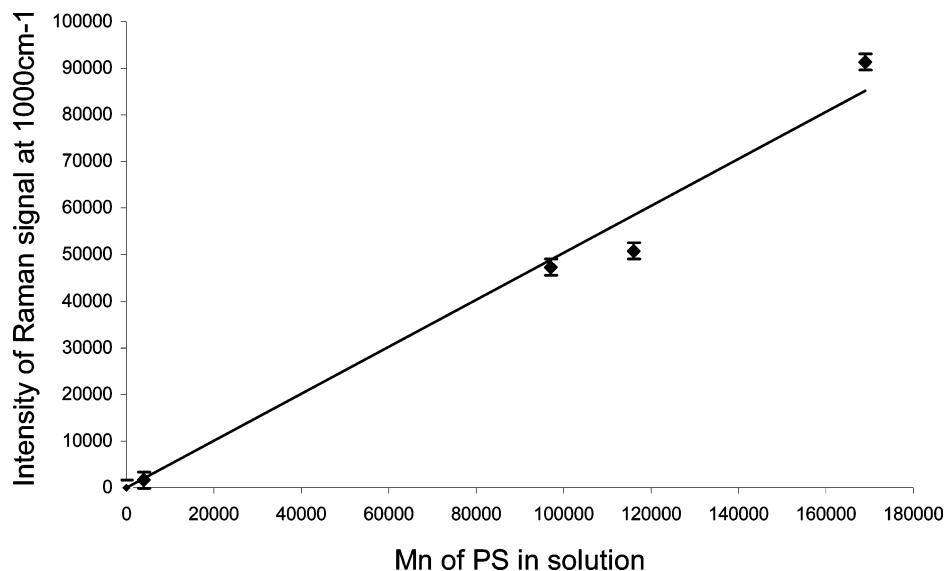


Figure 5. Plot of the Raman signal intensity for the peak at 1100 cm^{-1} vs M_n of the grafted PS chains measured by SEC.

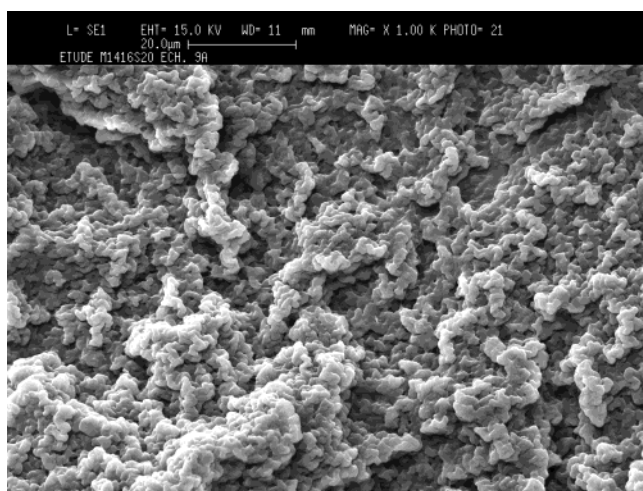


Figure 6. SEM image for PS grafted steel.

Contact angle measurements show an increase in the surface hydrophobicity when styrene is polymerized from the surface of poly(cPEA)-modified steel. The contact angle of water is indeed 85° compared to 73° for the poly(cPEA) surface. Moreover, 85° is the value measured for a polystyrene cast film.

The adhesion strength is another representative property for the grafting of PS to the surface. The energy required to peel a standard scotch tape (3M-acrylic foam 4930) was measured. The peeling energy from neat steel is 1850 N/m . This value increases up to 2340 N/m when PS is grafted by the strategy under consideration. This energy is, however, the adhesive energy between PS and the tape because the adhesive rupture occurs at this interface. The actual adhesive energy of PS onto steel is thus higher than 2340 N/m . The same test was repeated for steel grafted by poly(cPEA), thus before styrene polymerization. The energy is then 2270 N/m , the Scotch brand tape being again detached from the polymer coating.

Figure 6 shows the scanning electron micrograph (SEM) for the steel surface after styrene polymerization. The surface is completely coated by PS. As previously mentioned and confirmed by atomic force microscopy (AFM), the film is very rough, which prevents the thickness from being measured by ellipsometry. The

AFM can be equipped with a probe, which provides information on both the morphology and the thermal properties of the surface. Microthermal analysis (μ TA) consists of a tiny resistive thermal probe that collects images in relation to the sample topography and thermal conductivity.²⁴ The AFM tip is an ultraminiaturized resistive heater and a temperature sensor. Moreover, when an image is recorded, it is possible to select locations on the surface for further examination by local thermal analysis (LTA). The probe is positioned at one selected point, and the temperature is ramped between two predetermined limits at a rate ($5\text{--}25\text{ }^\circ\text{C/s}$), which is very high compared to traditional thermal analysis. When the polymer sample is softening, the thermal probe tends to penetrate the film and the displacement is detected by the position-sensitive detector of the AFM apparatus. Moreover, since the contact area between the tip and the material increases with time, the thermal power required for the scanning temperature diverges compared to the reference signal recorded in air. These measurements thus allow detecting thermal transitions on the local scale, even for thin films. It must be noted, however, that the technique is primarily sensitive to the softening of the polymer, which is related to the viscosity. Although the recorded transition cannot be strictly assimilated to T_g , the LTA curves can be used to compare a series of polymers. The transition measured by LTA in this study will be discussed on a comparative basis for PS either grafted to or solvent cast on steel. Figure 7a shows typical LTA curves collected for a polystyrene film (reference sample) cast on steel from a THF solution. The curves are the derivative of the power vs temperature, with endotherms pointing up. The endotherm at $137\text{ }^\circ\text{C}$ is the signature of the softening of PS. It must be noted that LTA performed at different locations of the same PS film is reproducible, as illustrated by the five curves in Figure 7a. Figure 7b compares the LTA curves recorded for a solvent-cast PS film and for PS grafted on steel. It is clear that the softening point of grafted PS is increased by ca. $10\text{ }^\circ\text{C}$ compared to the solvent-cast film. This difference may reflect a loss of mobility when one end of the PS chains is immobilized at the solid substrate.^{25–26} Difference in the molecular weight of the PS chains ($M_n = 175\text{ }000$ for solvent-cast PS, and $100\text{ }000$ for grafted chains) and

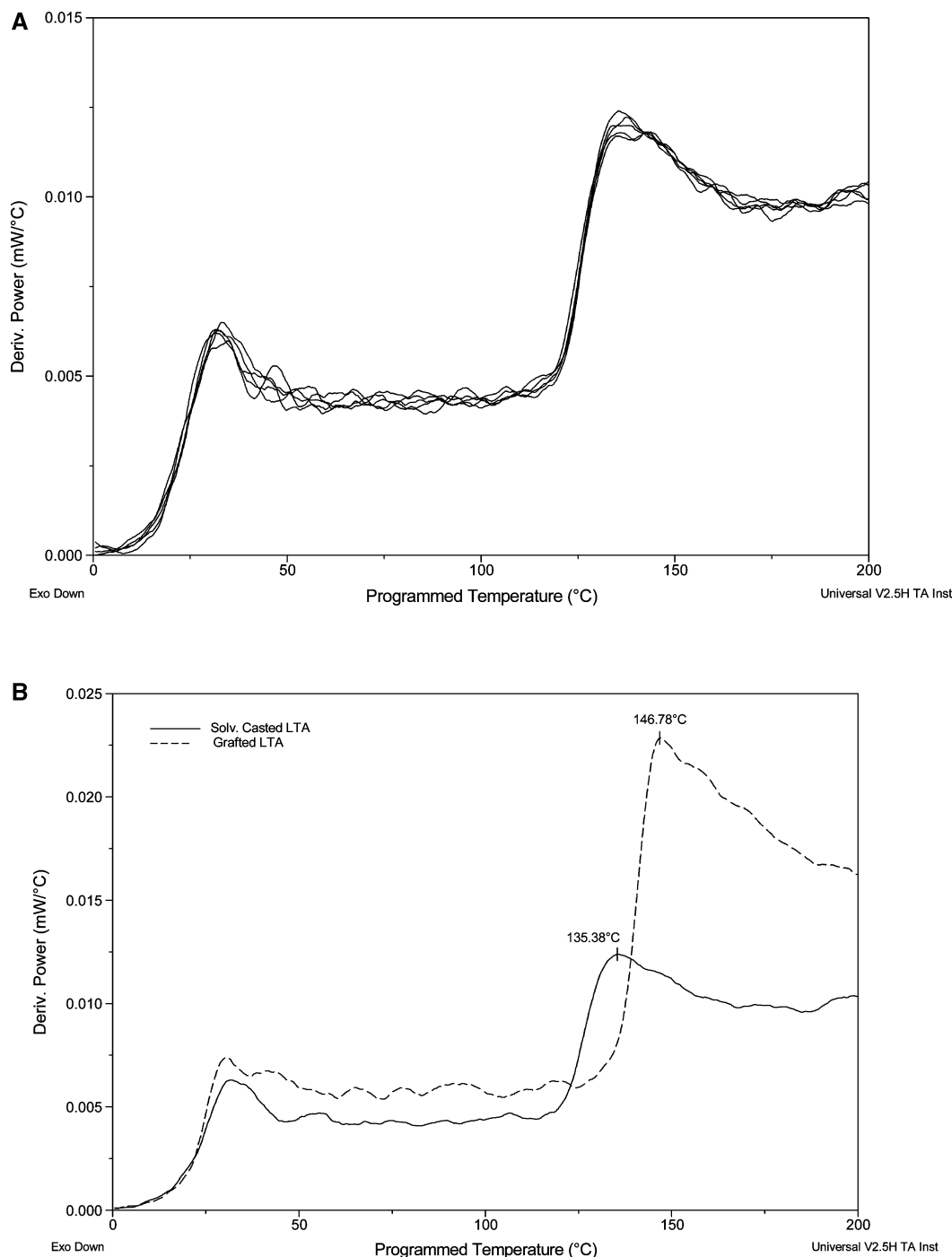


Figure 7. (a) LTA curves for a PS film solvent-cast on steel. The curves correspond to five locations on the film. These curves are the derivatives of the power vs temperature, with endotherms pointing up. (b) LTA curves for PS films prepared on steel. PS solvent-cast onto steel (solid line); PS grafted onto steel (dashed line).

in their viscosity cannot account for the transition temperatures observed in Figure 7a. The peak at 147 °C thus appears as the thermal signature of the PS grafting. Above the softening temperature, the LTA tip gradually penetrates the film and the vertical displacement of the probe can give a very rough estimation of the film thickness. Thicknesses from 200 nm to few micrometers was estimated in relation to the styrene/PEBr molar ratio used in the “grafting-from” step.

Conclusions

Combination of electrografting of a chlorinated acrylate and ATRP of styrene is a powerful tool to modify the surface of steel by strongly adhering PS chains.

Even though activated chlorine is not completely stable under the cathodic potentials used for the electrografting of the parent acrylate, ca. 90% of the theoretical chlorine content is preserved and available to the “grafting-from” of polystyrene by ATRP. The electrografting of the ATRP macroinitiator is responsible for the strong adhesion of polystyrene formed afterward. Although the control of the radical polymerization that occurs at the surface might be improved, polystyrene films strongly adhering to steel were deposited by this method, which is not possible by direct electrografting of styrene. Moreover, molecular weight of grafted PS and film thickness can be changed by the monomer/alkyl halide (in solution) molar ratio. Very adherent polysty-

rene films with thicknesses ranging from 200 nm to 1 μm can be deposited onto steel. As compared to the previously reported NMP process, combination of electrografting and ATRP has the drawback to be less controlled for styrene polymerization conducted in the presence of the Grubbs catalyst, which was used for inertness toward steel. Whenever more stable substrates (e.g., carbon and noble metals), tolerate the copper-based catalytic system, the macromolecular parameters of the "grafted-from" polystyrene are much better controlled. As a rule, ATRP is more promising than NMP because the dual acrylate (cPEA) is of a much easier synthesis than the alkoxyamine bearing the acrylate, and the range of monomers polymerizable by ATRP is broader.

Acknowledgment. The authors are much indebted to the "Service Fédéraux des Affaires Scientifiques, Techniques et Culturelles" for general support under the auspices of the "Pôles d'Attraction Interuniversitaires: Supramolecular Chemistry and Supramolecular Catalysis (PAI V/3)". Research in Mons was also partly supported by the European Commission, the Government of the Région Wallonne (FEDER-PHASING OUT) and the Belgian National Fund for Scientific Research (FNRS/FRFC). R.L. is Directeur de Recherche and C.J. is Chercheur Qualifié, près du Fonds National de la Recherche Scientifique (FNRS—Belgium). M.H. and R.G. thank the European Community and the "Ministère de la Région wallonne" for financial support. S.V. thanks the "Fonds pour la Formation à la Recherche dans l'Industrie et dans l'Agriculture (FRIA)" for a fellowship.

References and Notes

- (1) Guny, G.; Cao, J.; Hauske, J. *Tetrahedron Lett.* **1997**, *38*, 5237.
- (2) Velten, U.; Tossati, S.; Shelden, R.; Caseri, W.; Suter, U. *Langmuir* **1999**, *15*, 6940.
- (3) Kariuki, J.; McDermott, T. *Langmuir* **1999**, *15*, 6534.
- (4) Tanguy, J.; Deniau, G.; Augé, C.; Zalczer, G.; Lecayon, G. *J. Electroanal. Chem.* **1994**, *377*, 115.
- (5) Baute, N.; Teyssié, P.; Martinot, L.; Mertens, M.; Dubois, P.; Jérôme, R.; *Eur. J. Inorg. Chem.* **1998**, 1711. Baute, N.; Calberg, C.; Dubois, P.; Jérôme, C.; Jérôme, R.; Martinot, L.; Mertens, M.; Teyssié, P. *Macromol. Symp.* **1998**, *134*, 157.
- (6) Delamar, M.; Désarmot, G.; Fagebaume, O.; Hitmi, R.; Pinson, J.; Savéant, J. M. *Carbon* **1997**, *35*, 801.
- (7) Yuan, W.; Iroh, J. O. *Trends Polym. Sci.* **1993**, *1*, 388.
- (8) Baute, N.; Martinot, L.; Jérôme, R. *J. Electroanal. Chem.* **1999**, *472*, 8.
- (9) Detrembleur, C.; Jérôme, C.; Claes, M.; Louette, P.; Jérôme, R. *Angew. Chem., Int. Ed. Engl.* **2001**, *40*, 1268–1271.
- (10) Schwab, P.; France, M.; Ziller, J.; Grubbs, R. *Angew. Chem., Int. Ed. Engl.* **1995**, *34*, 2039.
- (11) Voccia, S.; Jérôme, C.; Detrembleur, C.; Gouttebaron, R.; Hecq, M.; Gilbert, B.; Jérôme, R. *Chem. Mater.*, in press.
- (12) Matyjaszewski, K.; Patten, T. E. *Adv. Mater.* **1998**, *10*, 12.
- (13) Moad, G.; Solomon, D. H. *The Chemistry of Free Radical Polymerization*; Pergamon: Oxford, England, 1995.
- (14) Matyjaszewski, K. *J. Macromol. Sci. Pure Appl. Chem.*, **1994**, *A31*, 989.
- (15) Curran, D. P. *Synthesis* **1988**, 489.
- (16) Wang, J. S.; Matyjaszewski, K. *J. Am. Chem. Soc.* **1995**, *117*, 5614.
- (17) Mertens, M.; Calberg, C.; Martinot, L.; Jérôme, R. *Macromolecules* **1996**, *29*, 4910.
- (18) Mertens, M.; Calberg, C.; Baute, N.; Jérôme, R.; Martinot, L. *J. Electroanal. Chem.* **1998**, *441*, 237.
- (19) Jérôme, C.; Geskin, V.; Lazzaroni, R.; Bredas, J. L.; Thibaut, A.; Calberg, C.; Bodart, I.; Mertens, M.; Martinot, L.; Rodrigue, D.; Riga, J.; Jérôme, R. *Chem. Mater.* **2001**, *13*, 1656–1664.
- (20) Jeyaparakash, J. D.; Samuel, S.; Dhamodharan, R.; Rühe, J. *Macromol. Rapid Commun.* **2002**, *23*, 277. Zhao, B.; Brittain, W. J. *Prog. Polym. Sci.* **2000**, *25*, 677.
- (21) Simal, F.; Delaude, L.; Jan, D.; Demonceau, A.; Noels, A. F. *Polymer Preprint* **1999**, *40*, 336.
- (22) Simal, F.; Demonceau, A.; Noels, A. F. *Tetrahedron Lett.* **1999**, *40*, 5689.
- (23) Simal, F.; Demonceau, A.; Noels, A. F. *Angew. Chem., Int. Ed.* **1999**, *38*, 4.
- (24) Song, M.; Hammiche, A.; Pollock, H. M.; Hourston, D. J.; Reading, M. *Polymer* **1995**, *36*, 3313. Song, M.; Hourston, D. J.; Reading, M.; Hammiche, A.; Pollock, H. M. *Polymer* **1996**, *37*, 243. Reading, M.; Hourston, D. J.; Song, M.; Pollock, H. M.; Hammiche, A. *Am. Lab.* **1998**, *Jan.*, 13. Price, D.; Reading, M.; Hammiche, A.; Pollock, H. M. *Int. J. Pharm.* **1999**, *192*, 85.
- (25) Keddie, J. L.; Jones, R. A. L.; Cory, R. A. *Faraday Discuss.* **1994**, *98*, 219.
- (26) Nielsen, L.; Laudel, R. *Mechanical Properties of Polymers and Composites*, 2nd ed.; M. Dekker: New York, 1994; p 20.

MA0217130